Inorg. Chem. **2009**, *48*, 1811−1818

Optical and Electrochemical Properties of Shell−Core Dendrimers: Ruthenium Coordination Complexes Capped with Sized Phenothiazine-substituted Bipyridines

Linyong Zhu, Douglas Magde, James K. Whitesell,* and Marye Anne Fox*

Department of Chemistry and Biochemistry, University of California at San Diego, 9500 Gilman Drive, La Jolla, California 92093-0358

Received May 27, 2008

A family of ruthenium coordination compounds capped by 4,4′-dimethylbipyridine ligands bearing 0, 1, 2, and 3 generations of dendritic phenothiazine moieties exhibit size-dependent electrochemical properties and structure-dependent absorption and luminescence spectra. Emission quantum yields, photoluminescence decay kinetics, and transient absorption spectra varied roughly with dendrimeric size and complexity on timescales from subnanoseconds to milliseconds. All complexes exhibit microsecond-lived lowest lying metal-to-ligand charge transfer excited states. Luminescence spectra were broadened compared with the unsubstituted parent, and quantum yields of emission for the large dendritic clusters were reduced by factors of two to five. Although the observed decay kinetics were complex, one transient decayed rapidly on a nanosecond scale, and a second intermediate showed no decay over a time scale of several tens of nanoseconds. Transient absorption measurements showed ground-state bleaching in regions of high ground-state absorptivity by the metal-to-ligand charge-transfer transient, as well as transient absorption shifts characteristic of isolated phenothiazine and ruthenium bipyridyl moieties.

1. Introduction

Photoexcitation of multichromophores arranged as molecular antennas can induce efficient long-lived charge separation in molecules bearing donor−acceptor pairs.[1] Such arrays are efficient light harvesters[2] that can lead to photoinduced formation of electron−hole pairs by interfacial electron injection when the light collecting arrays are bound to the surfaces of semiconductor films.[3] The long lifetimes of the resulting electron−hole pairs have attracted attention for decades.[4−9]

A thorough understanding of energy partitioning in macromolecules bearing multiple chromophores is also key to the development of artificial photosynthetic arrays[10] and to the utilization of multicomponent ordered arrays[11] with optical or electrical gradients.[12] The latter are required for the design of molecular computers.[13] Understanding the effect of aggregation and excited-state complexation on the kinetics of energy and electron transfer in integrated nanoscopic arrays is also of vital importance in attempts to duplicate the high efficiency of natural multichromophoric systems. Recent structural work has shown that tens of center.[14] Delineation of the photophysical properties of such arrays is admittedly difficult, but the practical importance of such arrangements nonetheless calls for such investigations even if the system complexity precludes full and clean optical characterization.

* To whom correspondence should be addressed. E-mail: mafox@ucsd.edu (M.A.F.), jkw@ucsd.edu (J.K.W.).

(1) Vlcek, A., Jr. In *Electron Transfer in Chemistry*; Balzani, V., Ed.; Wiley-VCH: New York, 2001; Vol. 2, pp 804−877, and references therein.
(2) (a) Meyer, T. J. *Acc. Chem. Res.* **1989**, *22*, 163. (b) Thompson, D. W.; Fleming, C. N.; Myron, B. D.; Meyer, T. J. *J. Phys. Chem. B* **2007**, *111*, 6930. (c) Taranekar, Q. Q.; Jiang, H.; Schanze, K. S.; Reynolds, J. R. *J. Am. Chem. Soc.* **2007**, *129*, 8958.
(3) (a) Grätzel, M. *Inorg. Chem.* **2005**, *44*, 6841. (b) Hoertz, P. G.; Staniszewski, A.; Marton, A.; Higgins, G. T.; Incarvito, C. D.; Rheingold, A. L.; Meyer, G. J. *J. Am. Chem. Soc.* **2006**, *1281*, 8234.
(4) Gust, D.; Moore, T. A.; Moore, A. *Acc. Chem. Res.* **2001**, *34*, 40.
(5) Haque, S. A.; Handa, S.; Peter, K.; Palomares, E.; Thelakkat, M.; Durrant, J. R. *Angew. Chem., Int. Ed.* **2005**, *44*, 5740.
(6) Argazzi, R. A.; Bignozzi, C. A.; Heimer, T. A.; Castellano, F. N.; Meyer, G. J. *J. Phys. Chem. B* **1997**, *101*, 2591.
(7) Odobel, F.; Zabri, H. *Inorg. Chem.* **2005**, *44*, 5600–5611.
(8) Wasielewski, M. R. *Chem. Rev.* **1992**, *92*, 435.
(9) Balaban, T. S. *Acc. Chem. Res.* **2005**, *38*, 612.
(10) Fox, M. A. *Acc. Chem. Res.* **1992**, *25*, 569.
(11) Watkins, D. M.; Fox, M. A. *J. Am. Chem. Soc.* **1996**, *118*, 4344.
(12) Watkins, D. M.; Fox, M. A. *J. Am. Chem. Soc.* **1994**, *116*, 6441.
(13) Gust, D.; Moore, T. A. *Science* **1989**, *244*, 35.
(14) Kühlbrandt, W.; Wang, D. N.; Fujiyoshi, Y. *Nature* **1994**, *367*, 614.

10.1021/ic800965p CCC: $40.75
Published on Web 01/27/2009

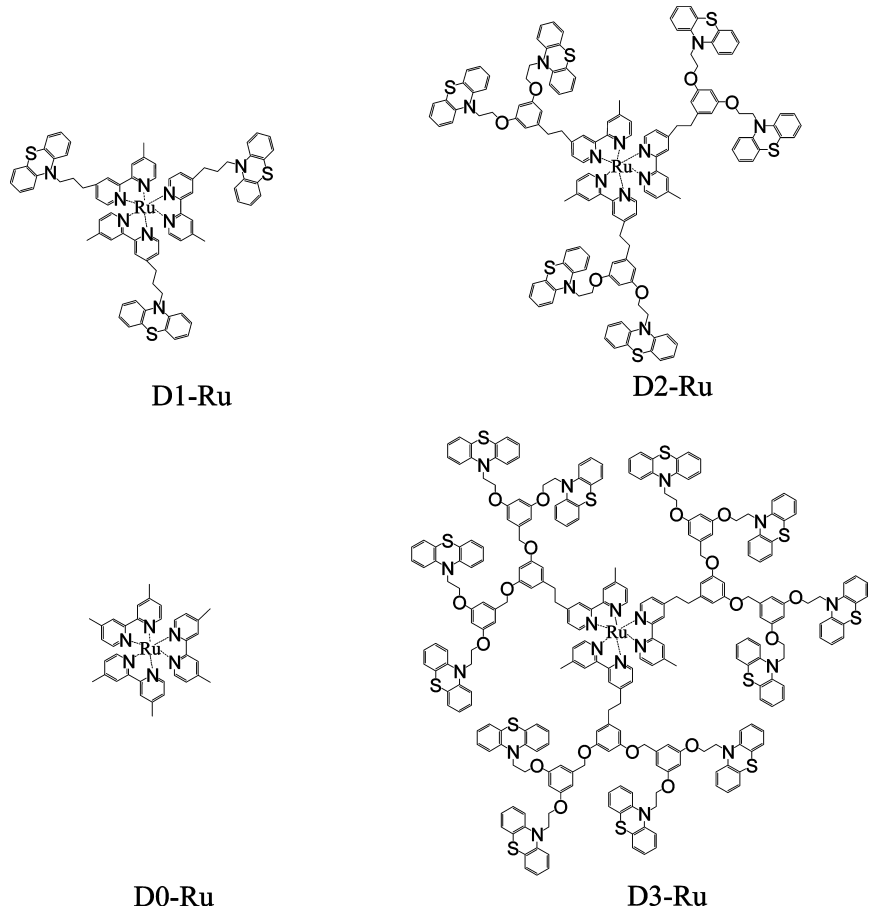

Figure 1. Structures of the ruthenium (II) dendrimer (D-A) dyads.

One-, two-, or three-dimensional arrays of multiple appended dyes bound to a redox complex can be devised to test the effect of order and absorptivity in these applications. For solar energy conversion applications, where efficiency is of great concern, even incremental improvements in charge separation, yield, and lifetime can be critical.[15] Shell−core dendrimers bearing multiple chromophores at the periphery[16] may be excellent contributors to enhanced solar conversion if the intramolecular excited-state properties of such families are better understood.

Dendritic antennas are now synthetically accessible,[17−19] but fundamental characteristics of the photophysical response to anchoring multichromophore arrays of varying size and complexity to a core center have been incompletely determined to date. In this work, we described the synthesis and excited-state characterization of a series of ruthenium tris-bipyridyl complexes bearing 0, 3, 6, or 12 phenothiazine dyes, Figure 1. We address the basic photophysical characteristics of this family, seeking to determine the feasibility of employing the resulting excited-state properties of this family as stable, highly absorptive, nanoscaled photosensitizers to be used as important components of next-generation solar cells.

Intramolecular photophysics of tris-bipyridyl ruthenium was first described in a seminal contribution of Klassen and Crosby,[20] and intermolecular charge transfer from a relatively long-lived triplet excited-state has been well documented by Gafney and Adamson.[21] Comprehensive reviews of the photophysical properties of derivatives of this family show these compounds to be important donors and acceptors likely to be useful in practical photocells.[21,22]

To extend these studies, we synthesized ruthenium[II] complexes containing up to three dendrimer generations of phenothiazine moieties appended to a redox-active Ru[II]core via well-known bipyridine linking ligands. Our target molecules are illustrated in Figure 2 and are identified as **D0**, **D1**, **D2**, and **D3**, where the number refers to the dendrimer generation. The corresponding uncomplexed ligands are identified respectively as **L0** to **L3**. As a family, these compounds differ from previously reported arrays in containing multiple ultraviolet absorbing units bridged by a dendritic connector to a single one-electron trap.[20−23,25] We report here fundamental photophysical and electrochemical

(15) El-Khouly, M. E.; Kang, E. S.; Kay, K.-Y.; Choi, C. S.; Aaraki, Y.; Ito, O. *Chem.—Eur. J.* **2007**, *13*, 2854.
(16) Jiang, D.-L.; Aida, T. *Nature* **1997**, *388*, 454–456.
(17) Zhu, L. Y.; Tong, X. F.; Li, M. Z.; Wang, E. J. *J. Phys. Chem. B* **2001**, *105*, 2461–2464.
(18) Stewart, G. M.; Fox, M. A. *J. Am. Chem. Soc.* **1996**, *118*, 4354–4360.
(19) Crosby, G. A.; Perkins, W. G.; Klassen, D. M. *J. Chem. Phys.* **1965**, *43*, 1498.
(20) Gafney, A. D.; Adamson, A. W. *J. Am. Chem. Soc.* **1972**, *94*, 8238.
(21) Juris, A.; Balzani, V.; Barigelletti, F.; Campagna, S.; Belser, P.; von Zelewsky, A. *Coord. Chem. Rev.* **1988**, *84*, 85.
(22) Balzani, V.; Bergamini, G.; Marchioni, F.; Ceroni, P. *Coord. Chem. Rev.* **2006**, *250*, 1254.
(23) Ciana, L. D.; Hamachi, I.; Meyer, T. J. *J. Org. Chem.* **1989**, *54*, 1731.
(24) Hawker, C. J.; Fréchet, J. M. J. *J. Am. Chem. Soc.* **1990**, *112*, 7638.

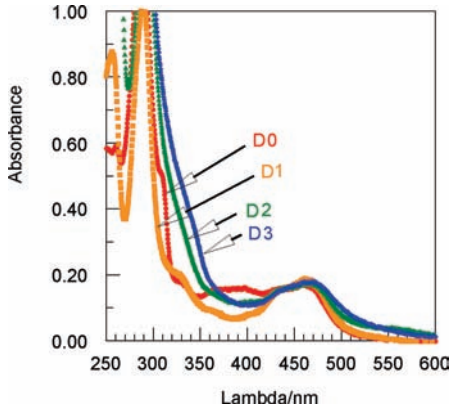

Figure 2. Steady state absorption for four ruthenium compounds, the parent and three dendrimers, in dichloromethane. These are the same specific solutions used to generate Figure 3.

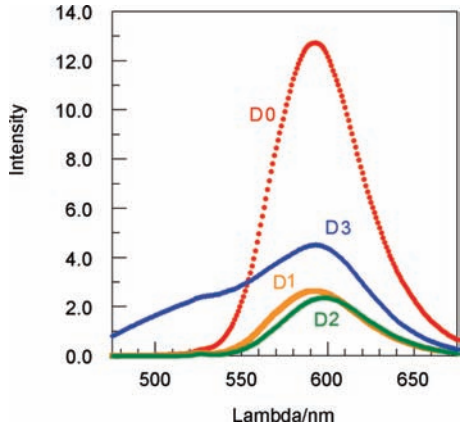

Figure 3. Steady state luminescence spectra for four ruthenium compounds in air-saturated dichloromethane. All four had the same absorption at the excitation wavelength of 355 nm.

properties of these homoleptic complexes, which have three identical ligands bound through an substituted 4,4′-dimethylbipyridyl-bis-carboxylate ligand and one to three generations of phenothiazine (PTZ) dyes.

2. Experimental Section

Chemicals. All chemicals were purchased from Aldrich. Potassium carbonate (K_2CO_3) was dried in an oven at 130 °C. Dichloromethane (CH_2Cl_2) and tetrahydrofuran (THF) were distilled from CaH_2 and sodium/benzophenone, respectively. All other reagents were used as received. NMR spectra were recorded in $CDCl_3$ and are reported in ppm versus TMS.

10-(2-Chloroethyl) phenothiazine, 10-(2-bromoethyl) phenothiazine (G1-Br) and 10-[3-(4-methyl-2, 2′-bipyridine-4yl)propyl] phenothiazine (L1-Bpy) were prepared using the methods of Meyer et al.[23]

Synthesis. The general strategy for the synthesis of the dendrimers followed procedures developed by Fréchet et al.[24] for the conversion of alcohol dendrons to the corresponding bromides (Scheme 1). For the preparation of the dendritic bipyridine ligands, 4,4′-dimethyl-2,2′-bipyridine (Me_2bpy) was treated with an excess of LDA in dry THF at −78 °C to give the orange lithiated derivative. After 45 min, the dendritic benzyl bromides, dissolved in minimal dry THF, were added to the reaction mixture, resulting in the desired monosubstituted dendritic bipyridine ligands.

The first, second, and third generation ruthenium dendrimers, **Dn-Ru ($n = 1, 2,$ and 3)** were prepared by the complexation of ruthenium trichloride and the respective bipyridine ligand in a chloroform/ethanol mixture while being heated at reflux for 4 days. The chloride salts of the ruthenium dendrimers were quite soluble in CH_2Cl_2 and THF, presumably because of the highly branched organic groups dispersed around the ruthenium−metal center. Because the series of compounds were highly hygroscopic, analysis by mass spectral measurement proved to be the preferred analytical technique.

Preparation of the Benzyl Alcohol Dendrons [Gn-OH] ($n = 2, 3$), Scheme 1. The respective benzyl bromide dendron (2.1 equiv), 3,5-dihydroxybenzyl alcohol (1.0 equiv), K_2CO_3 (5 equiv), and 18-crown-6 (0.5 equiv) were heated to reflux in minimum acetone for 48 h. The solvent was removed under vacuum, and the residue was dissolved in CH_2Cl_2, washed with water (3×), and then dried over anhyd. Na_2SO_4. The solution was concentrated under vacuum and chromatographed on a silica gel column. The product was eluted with CH_2Cl_2 to yield a faintly yellow crystalline solid. Yield 40−70%.

[G2-OH]. ^{1}H NMR ($CDCl_3$) δ: 4.28 (s, 8 H), 4.56 (s, 2 H), 6.36 (d, 1 H), 6.51 (d, 2 H), 6.93 (m, 8 H), 7.15 (m, 8 H). Mass-EI: Calcd for $C_{35}H_{30}N_2O_3S_2$, m/z 590.17, Found: 590.13.

[G3-OH]. ^{1}H NMR ($CDCl_3$) δ: 4.26 (s, 16 H), 4.59 (s, 2 H), 4.89 (s, 4 H), 6.37 (s, 2 H), 6.44 (s, 1 H), 6.58 (m, 6 H), 6.82−6.98 (m, 16 H), 7.05−7.20 (m, 16 H). Mass-EI: Calcd for $C_{77}H_{64}N_4O_7S_4$, m/z 1284.37. Found: 1284.32.

Preparation of the Benzyl Bromide Dendrons [Gn-Br] ($n = 2, 3$), Scheme 1. To the respective benzyl alcohol dendron (1.0 equiv) in a minimum of THF was added CBr_4 (2.5 equiv). The solution was stirred for 5 min before the addition of PPh_3 (2.5 equiv). The solution was stirred under Ar for 1 h, after which the solvent was removed under vacuum. The remaining solid was dissolved in CH_2Cl_2 and extracted (3×) with water. The organic layer was dried over anhyd. Na_2SO_4 and concentrated under vacuum, before being applied to a silica column and eluted with CH_2Cl_2/hexane (4:1), and then washed by ethyl ether. Yield 60−70% as a white powder.

[G2-Br]. ^{1}H NMR ($CDCl_3$) δ: 4.27 (s, 8 H), 4.35 (s, 2 H), 6.36 (d, 1 H), 6.53 (d, 2 H), 6.87−7.02 (m, 8 H), 7.10−7.20 (m, 8 H). Mass-EI: Calcd for $C_{35}H_{29}BrN_2O_2S_2$, m/z 652.09. Found: 652.09.

[G3-Br]. ^{1}H NMR ($CDCl_3$) δ: 4.26 (s, 18 H), 4.87 (s, 4 H), 6.35 (d, 2 H), 6.43 (s, 1 H), 6.55(s, 6 H), 6.85−6.98 (m, 16 H), 7.06−7.20 (m, 16 H). Mass-EI: Calcd for $C_{77}H_{63}BrN_4O_6S_4$, m/z 1346.28. Found: 1346.25.

Preparation of [L2-Bipy] and [L3-Bipy], Scheme 1. BuLi (2.5 M in hexanes, 2.25 equiv) was added to a solution of diisopropyl amine (2.25 equiv) in a small amount of THF, and the resulting mixture was stirred for 15 min at −78 °C in a dry ice-acetone bath under argon. 4,4′-dimethyl-2,2′-bipyridine (1.25 equiv) dissolved in a minimum amount of THF was then added from a dropping funnel. After 2 h, **Gn-Br** (1.0 equiv) in minimal THF was added to the solution. During an additional 1 h of stirring, the solution was allowed to slowly warmed to room temperature and was then stirred overnight. The reaction mixture was quenched with water and extracted with CH_2Cl_2 (3×). The organic layer was dried over anhyd. Na_2SO_4, and the solvent

(25) Puntoriero, F.; Nastasi, F.; Cavazzini, M.; Quici, S.; Campagna, S. *Coord. Chem. Rev.* **2007**, *251*, 536.

Scheme 1. Synthesis Procedures for Dendrimeric Ligands and Ruthenium (II) Complexes **1**−**5**[a]

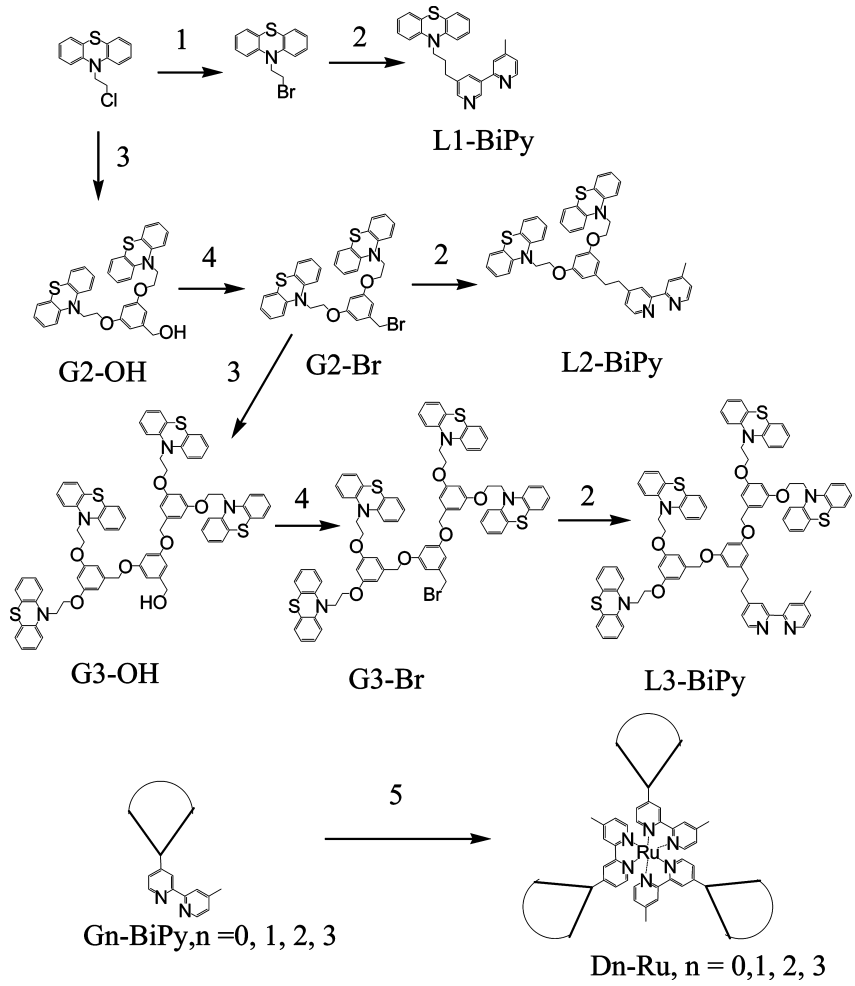

[a] **1:**NaBr, ethyl bromide and 1-methyl-2-pyrrolidinine, 65 °C; **2:** BuLi, diisopropyl amine and 4,4-dimethyl-2,2-bipyridine in THF, −78 °C; **3:** 3,5-dihydroxy benzyl alcohol, K_2CO_3, and 18-crown-6 in acetone reflux; **4:** CBr_4 and PPh_3 in THF, 25 °C; **5:** $RuCl_3 \cdot 3\ H_2O$ in 3:1 $CHCl_3$, ethanol reflux.

was removed under vacuum. The crude product was applied to a silica gel column and eluted with CH_2Cl_2, followed by 2−5% methanol in CH_2Cl_2. Yield 40−50%.

[L2-bpy]. ^{1}H NMR ($CDCl_3$) δ: 2.44 (s, 3 H), 2.88 (t, 2 H), 2.91 (t, 2 H), 4.26 (s, 8 H), 6.30 (d, 1 H), 6.37 (d, 2 H), 6.94 (m, 8 H), 7.15 (m, 8 H), 8.23 (s, 3 H), 8.54 (m, 3 H). Mass-EI: Calcd for $C_{47}H_{40}N_4O_2S_2$, *m*/*z* 756.26. Found: 756.25.

[L3-bpy]. ^{1}H NMR ($CDCl_3$) δ: 2.42 (s, 3 H), 2.51 (t, 2H), 2.52 (t, 2 H), 4.26 (s, 16 H), 4.88 (s, 4 H), 6.38 (s, 1 H), 6.40 (s, 2 H), 6.58 (m, 6 H), 6.82−6.98 (m, 16 H), 7.05−7.20 (m, 16 H), 8.23 (s, 3 H), 8.54 (m, 3 H). Mass-EI: Calcd for $C_{89}H_{74}N_6O_6S_4$, *m*/*z* 1450.46. Found: 1450.42.

Preparation of the Ruthenium Dendrimers [Dn-Ru] (*n* = 1, 2 and 3), Scheme 1. The respective dendron **[Gn-Bipy]** (3.0 equiv) and ruthenium trichloride hydrate (1.0 equiv) were heated to reflux in 3:1 $CHCl_3$:EtOH for 4 days. The solvent was then removed under vacuum, and the brown solid was loaded onto a silica gel column eluted with 20:1 CH_2Cl_2/MeOH. A bright orange solution was collected, and the solvent was removed under vacuum to afford the ruthenium dendrimer.

[D1-Ru] Dendrimer. Yield 72%, ^{1}H NMR ($CDCl_3$) δ: 2.20 (m, 6 H), 2.49 (s, 9 H), 2.78(t, 6 H), 3.91 (t, 6 H), 6.84−7.28 (b, 24 H), 8.51 (m, 9 H), 8.82 (m, 9 H), MALDI (matrix: DHB), *m*/*z* [M − 2Cl]$^{2+}$ Calcd for $C_{78}H_{69}N_9RuS_3$ 1329.39. Found 1329.1.

[D2-Ru] Dendrimer. Yield 40%, ^{1}H NMR ($CDCl_3$) δ: 2.47 (s, 9 H), 2.82−3.05 (b, 12 H), 4.36 (s, 24 H), 6.38−6.51 (m, 9 H), 6.99 (b, 24 H), 7.20 (b, 24 H), 8.28 (s, 9 H), 8.62 (m, 9 H). MALDI (matrix: DHB), *m*/*z* [M − 2Cl] $^{2+}$ Calcd for $C_{141}H_{120}N_{12}O_6RuS_6$ 2370.68. Found 2370.3.

[D3-Ru] Dendrimer. Yield 12%,^{1}H NMR ($CDCl_3$) δ: 2.44 (s, 9 H), 2.53−2.60 (m, 12 H), 4.28 (s, 48 H), 4.98 (s, 12 H), 6.36−6.70 (b, 27 H), 6.85−7.01 (b, 48 H), 7.03−7.35 (m, 48 H), 8.29 (s, 9 H), 8.54 (m, 9 H). MALDI (matrix: DHB), *m*/*z* [M − 2Cl] $^{2+}$ Calcd for $C_{267}H_{222}N_{18}O_{18}RuS_{12}$ 4453.27. Found 4453.4.

Steady-State Absorption and Luminescence. All measurements were recorded as deaerated dichloromethane solutions at ambient temperature. Absorption spectra were measured using an Ocean Optics spectrophotometer. Luminescence was measured on a Jasco FP-6200 spectrofluorimeter.

Time-Resolved Emission. Lifetimes reported here were obtained using a nanosecond laser with excitation at 355, 455, or 532 nm. The solutions were sparged gently with argon for 20−30 min before each measurement to remove oxygen. The monochromator used a 10 nm bandpass; glass filters were added to eliminate scattered excitation light. (Raman scattering could interfere in some cases, albeit with a much shorter lifetime.) An Amperex TUVP56 photomultiplier tube designed to sustain linear anodic currents produced signals that were read on a LeCroy 9361 digital oscilloscope. Curve fitting by a nonlinear least-squares method was carried out with in-house software. A femtosecond laser with time-correlated photon counting and deconvolution was used to obtain

Table 1. Electrochemical Potentials $E_{1/2}$,[b] Luminescence Yields in Aerated Solutions, and Fits to Luminescence Decay in Deaerated Solutions of Four Ruthenium(II) Compounds in Dichloromethane Solution at Ambient Temperature[a]

	$E_{1/2}$/Volt ± 0.1 V		quantum yield ± 0.03	decay, fraction(τ/ns)		
	$PTZ^{+/0}$	$Ru^{3+/2+}$	λ_{ex} = 455 nm	λ_{ex} = 355 nm	λ_{ex} = 455 nm	λ_{ex} = 532 nm
D0		1.10	0.120	1.00(805)	1.00(790)	1.00(795)
D1	0.61	1.27	0.025	0.80(75) + 0.20(900)	0.86(69) + 0.14(900)	0.80(74) + 0.20(890)
D2	0.62	1.25	0.022	0.33(104) + 0.51(350) + 0.16(870)	0.38(89) + 0.51(295) + 0.13(780)	0.33(86) + 0.50(287) + 0.17(760)
D3	0.67 (irr)	1.29 (irr)	0.070	0.39(154) + 0.61(445)	0.36(130) + 0.64(445)	0.45(185) + 0.55(480)

[a] See text for further explanation. [b] $E_{1/2}$ value +0.31 V vs SSCE; with $Fc^{+/0}$. Irr = irreversible

time resolution as short as 10 ps. All measurements refer to deaerated dichloromethane solutions at ambient temperature.

Transient Absorption. Absorption changes following nanosecond flash photolysis were measured with the nanosecond apparatus sketched above, except that a probe beam traversed the sample and was detected by the photomultiplier. Nanosecond laser pulse fluxes were in the range 10−100 mJ cm^{-2}, about an order of magnitude more than for emission studies. The higher values were employed for green excitation because that wavelength was absorbed very weakly. The excitation and probe pulses were colinear. Available as probes were both a continuous tungsten halogen lamp and a pulsed xenon discharge arc (500 μs full width at half-max, usable for small signals over a range of about 10 μs). For any given time range, care was taken to optimize predigitization electronic filtering to maximize signal-to-noise without distorting the signal.

Electrochemistry. Cyclic voltammetry and differential pulse voltammetry were performed using a Bioanalytical Systems CV-50W potentiostat. Electrochemistry was performed in dichloromethane in the presence of 0.1 M tetrabutylammonium hexafluorophosphate (TBAH). The working electrode was a gold disk (3 mm diameter), the counter electrode was a platinum wire, and the reference electrode was a ferrocene/ferrocenium couple (+0.31 V vs SSCE). Voltammograms were generated at a sweep rate of 100 mV/s. The $E_{1/2}$ values were calculated as the average of the oxidative and reductive peak potentials, $(E_{p,a} + E_{p,c})/2$ against a saturated calomel standard electrode.

3. Results

Absorption and Luminescence. Absorption and luminescence spectra for the dendrimeric complexes are illustrated in Figures 2 and 3, respectively. The absorption spectra were as expected for a ruthenium complex: $\pi-\pi^*$ bands in the ultraviolet and metal-to-ligand charge transfer (MLCT) bands in the visible region. The absorption spectra in Figure 2 were obtained for the same samples used for the luminescence spectra shown in Figure 3, with absorbances matched at 455 nm. The larger dendrimers, which bear many more phenothiazine groups, exhibit much larger absorbance in the region around 250 nm. In principle, the dendritic ligands may act as antenna systems for the ruthenium center, but the enhanced absorption occurs at much too short a wavelength to expect efficient solar energy conversion. The enhanced complexity of the appended phenothiazines enhance the local polarity and hence the stability of the MLCT transition.

Luminescence spectra exhibit a substantial Stokes shift of the triplet MLCT emission. The spectra illustrated were excited at 455 nm as deaerated solutions optically matched at the excitation wavelength. From the known quantum yield for **D0**, the quantum yields for emission of **D1**, **D2**, and **D3** were found to be smaller by factors of approximately 0.21, 0.48, and 0.58. From the yield for **D0** in deaerated dichloromethane (0.12), [25] we obtain the values listed in Table 1.

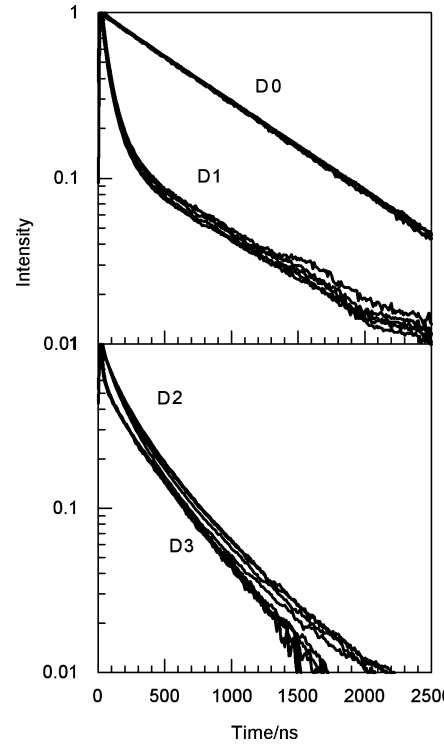

Figure 4. Luminescence decay for four ruthenium compounds, following excitation at 355 nm. In the top panel, each decay is an overlay of five wavelengths at 40 nm intervals. In the lower panel, four wavelengths are displayed for each compound.

A surprisingly broad emission spectrum for **D3** was probed by collecting the excitation spectra for **Dn** (n = **0−3**) for luminescence measured at 540 and 640 nm. The bands reflect complexity deriving from pi stacking in the excited-state of D2 and D3. For all four compounds, the observed excitation spectra were identical for both short and long emission wavelengths. This conclusion was also supported by time-resolved emission studies, as detailed below.

Luminescence Decay Kinetics. Figure 4 displays luminescence decay curves for the four Ru complexes in deaerated dichloromethane upon excitation at 455 nm, well within the MLCT absorption band. For each compound, luminescence decays were measured at several wavelengths between 570 and 730 nm, typically at 40 nm intervals. In the figure, the decays have been normalized and superimposed to emphasize that decay kinetics are independent of detection wavelength. There were no apparent systematic changes between the blue and the red ends of the emission spectra. Compound **D0** showed only the expected single exponential at all emission wavelengths, indicating that the observed decays emanate from the non-exponential behavior of the multiple phenothiazine derivatives. For compounds

D1, **D2**, and **D3**, multi-exponential decay is observed at every emission wavelength observed. Each decay might well be characterized by a continuum of rates, but for the precision available, each could be fit within statistical uncertainty using no more than three exponentials.

Decay kinetics were also measured upon excitation at 355 and 532 nm. If multiple species were present, and barring incredible coincidence, different excitation wavelengths should result in different decay kinetics. The results collected in Table 1 represent an average over fits for three to five emission wavelengths. The table displays lifetimes of each component of the fit in parentheses, as well as the fractional amplitude at time zero for each component. The listed fits imply no excitation transfer, which would have been evidenced as a discrete rise time. Rather, the observed decay is a superposition of features that begin at time zero and decay from there. Additional exponentials were included until the fit was not further improved significantly, that is, changed by less than a factor of 2 in chi-squared. For **D0**, the observed lifetime is approximately the same as for $Ru(bipy)_3$.[25]

The other compounds **D1**−**D3** all show a substantial fraction of a faster decay component throughout the emission. For **D1**, the decay is fit well to two exponentials, one similar to that of the parent and one that is faster. For **D2**, three components, at least, are needed, with a small fraction of the long-lived parent. For **D3**, two components suffice, within the available precision, mainly because the longest component has diminished to the point that it is no longer visible. The uncertainty (total range) in amplitude for fits at different wavelengths was generally no more than ±0.02. The variation in lifetimes for different trials at the same or different detection wavelengths was 1−2% for the single exponential fits of **D0**. For multiple exponential fits, the observed uncertainty depends on the total amplitude of emission. (It is more difficult to obtain excellent fits at the extremes of the emission range.) It also depends on the fractional contribution of the component transients, especially with three components (because the parameters are not statistically independent and are affected by minor amounts of instrumental noise). However, the net uncertainty in both amplitude and lifetime was again less than 5%.

The value for **D0** in Table 1 is about 100 ns shorter than was reported for the parent.[25] The critical point is that decays are clearly not single exponential for **D1**, **D2**, and **D3** and do not vary monotonically with either emission or excitation wavelength in any convincing manner. That some component of the observed emission decays more rapidly accounts for the reduced quantum yields of the more highly substituted derivatives.

Decay kinetics for samples equilibrated with air can be described as follows: **D0**displayed a perfect single exponential with a lifetime of 260 ns. The other compounds all required double exponential fits, with about half the decay occurring with a lifetime in the range of 50−100 ns. For **D2**, the fast component was at the short end of that range, and its fractional amplitude was quite large, near 80%. For **D2** and **D3**, the fast portion had a lifetime toward the longer end of the range and an amplitude of about one-third. Thus, the contributions of the longer lived species were reduced, as is consistent with the observed quantum yield results.

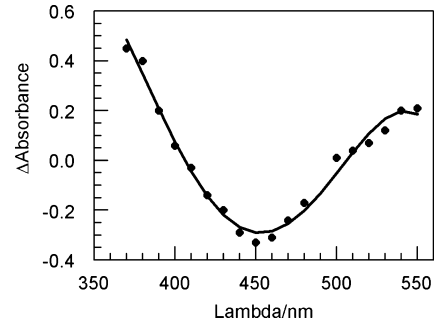

Figure 5. Transient absorption and bleaching is generally similar for all four ruthenium compounds.

The MLCT luminescence of all these compounds is relatively long-lived, even for the faster decay components of the dendrimers, when compared with decay times for typical organic dyes. The observed decay times correlate reasonably well with quantum yields, so there is little reason to suspect major contributions from even faster components. We searched, nevertheless, for any fast feature in the low nanosecond regime using time-correlated photon counting (TCPC) with excitation at 400 nm. It is difficult to detect with confidence a very short decay that is much smaller than a long-lived signal, since inevitable noise in the latter from photon statistics competes with any authentic signal, although it is quite easy to find large signals. At the same time, when enough sensitivity is attained upon near UV excitation, we can always find a very small residual signal with multiple lifetimes over the 1 to 3 ns range ascribed to trace organic impurities that absorb in the ultraviolet and near-UV.

Using picosecond methods, we observed only a very small impurity signal. Excitation at the available wavelength of 400 nm is not optimal from the standpoint of selecting for the MLCT emission and discriminating against the "universal trace impurities", but it does avoid any contribution from Raman scattering, which is generally much larger than our observed impurity effects. The excitation wavelength of 400 nm is too long to effect absorption in the phenothiazine or bipyridine moieties. Any direct excitation would be transferred very rapidly to the ruthenium center.

Transient Absorption. Transient absorption was investigated exhaustively. The transient spectrum displayed in Figure 5 is derived from kinetic traces and shows the absorbance at different wavelengths derived from fits extrapolated to zero time delay. The transient spectrum shows bleaching throughout a broad range centered near 450 nm, where ground-state MLCT absorption is prominent. Decay kinetics reveal that the transient in **D0** decays with a single exponential lifetime between 250 and 300 ns in deaerated solution, while **D1**, **D2**, and **D3** all decay with two lifetimes: one of 50−100 ns and a second near 300 ns. The transient spectra were obtained upon excitation at three wavelengths: 355, 455, and 530 nm. The last is useful for examining the blue-violet region; the second is useful for the orange-red region. Since the spectra are composites of different runs averaged together, there is some uncertainty in the amplitude

of the wings relative to midrange values. At the blue end, diminished instrument sensitivity is an issue; at the red end, there is minor concern about interference from luminescence. However, the general features were highly reproducible.

In addition to detecting transient absorption throughout the visible on the submicrosecond time scale, small amounts of a longer-lived feature ascribed to charge transfer to or from solvent was evident out to several seconds. Initial measurements revealed extremely small features in both absorption and bleaching, even when great care was taken to use optimal detection methods. Small signals (100 to 1000 times smaller than the peak of the transient spectrum) appeared for all excitation wavelengths but were most noticeable upon UV excitation at 355 nm, possibly because of subtle thermal lensing effects. Very slight inhomogeneities in the excitation beam or tiny misalignments can induce small fluctuations in the transmitted intensity. This is somewhat more problematic with UV excitation as it is more difficult to produce uniform excitation intensity over the probe region. Another possible artifact at the longest timescales was very slight photodegradation after hundreds of nanosecond pulses. We cannot exclude, on experimental grounds small, longer-lived transients deriving from authentic charge transfer, below the level of 1% of the initial features; but if any are present, they are minimal and do not interfere with the major spectral features observed.

Photophysical Properties of the Ligands Alone. The organic ligands **L0** to **L3** absorb in the mid-UV and emit fairly weakly in the near-UV to violet. Upon excitation with a 355 nm nanosecond pulse, we observed a fluorescence lifetime of about 1 ns, too short for decay analysis with the available apparatus. A transient absorption observed at all wavelengths from 380 to 600 nm, and persisting longer than the fluorescence, was assigned to a triplet state. No bleaching was observed in deaerated solution, which is to be expected without ground-state absorption in that region.

Electrochemistry. Cyclic voltammograms, Table 1, show that the isolated Ru (Me-bpy)$_3$ complex (**D0**) undergoes reversible oxidation ($Ru^{3+/2+}$) at +1.10 V. **D1**, **D2**, and **D3** display the expected $Ru^{3+/2+}$ wave but shifted to $E_{1/2} \approx 1.27$ V. The $PTZ^{+/0}$ wave appears at 0.61−0.67 V versus SSCE. Except for the third generation dendrimer, **D3**, the complexes display a reversible electrochemical oxidation, Figure 6. Thus, the observed oxidative cycle closely resembles that observed in analogous complexes in which bimetallic Os−Ru complexes in which dendritic phenothiazines are bound directly as donor subunits at the periphery.[25] The observed waves also establish the exoergonicity of electron transfer from an excited phenothiazine to the core Ru complex.

4. Discussion

Our characterization of the excited states of the dendrimer complexes focuses on features unique to dendrimers bearing multiple chromophores capable of charge transfer to an included redox partner. For such studies, it is important that the compounds be stable both thermally and photochemically.

The dendritic ligands themselves behave as expected: they absorb strongly in the UV but not in the visible. Upon flash photoexcitation at 355 nm, the family display a transient absorption throughout the visible with moderate intensity, as is expected for a triplet MLCT state or an oxidized phenothiazine. Ruthenium complexes of 4,4′-dimethylbipyridine and the three generations of dendrimers therefore provide an ideal family for probing three-dimensional multiabsorber integrated systems.

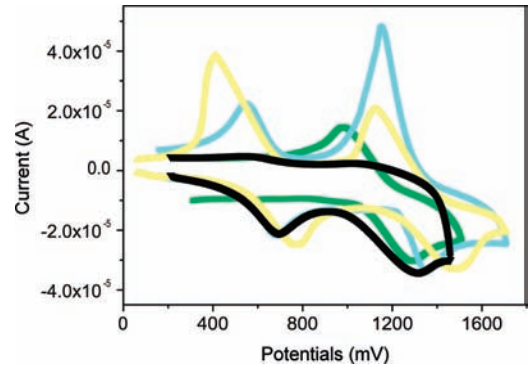

Figure 6. Cyclic voltammograms for four ruthenium compounds in dichloromethane with 0.1 M tetrabutylammonium hexafluorophosphate (TBAH); potentials are reported relative to ferrocene/ferrocenium: green, **D0**; blue, **D1**; yellow, **D2**; black, **D3**.

Compound **D0**, which lacks bound phenothiazines, exhibited the expected spectrum[26] and a single exponential luminescence decay. Compounds **D1**, **D2**, and **D3** all exhibit typical absorption with a broad triplet MLCT transition dominating the visible region. The dendritic family possesses characteristics not found in simpler parent compounds. The spectra are broader, particularly in **D3**, and the decay kinetics are multiexponential in all cases. Both features are likely caused by the extended dendritic ligands adopting a variety of conformations with differential coupling to the Ru core. That the spectrum is characteristic of a single complex, rather than a mixture of two different but well-defined species, is evidenced by the similarity of excitation spectra for luminescence resulting from excitation at widely different wavelengths within the broad emission profile. The observation that emission decay kinetics are similar throughout the emission spectrum and independent of excitation wavelength indicates the presence of a single emissive compound.

The fact that decay kinetics in progressively higher generation dendrimers are not single exponential proves that multiple emitting conformations exist. It is possible that individual molecules dispersed throughout the solvent may exhibit different radiative or non-radiative lifetimes. All emitting states, however, have characteristic MLCT states, as evidenced by both lifetime and spectral measurements. In homoleptic compounds, a range of different conformations are accessible in the chromophores appended to the increasingly large dendrimers. If the different states in question reside on different individual molecules, they would not be expected to transfer excitation efficiently to other species by diffusive encounter on that time scale. The different conformations of each emitting state, however, must not interconvert on the time scale of luminescence, that is, within one microsecond.

(26) Barigelletti, F.; De Cola, L.; Balzani, V.; Hage, R.; Haasnoot, J. G.; Reedijk, J.; Vos, J. G. *Inorg. Chem.* **1989**, *28*, 4344.

An interesting question is whether any given set of conformations for its three dendritic ligands might host multiple excited states with different decay rates. There has been evidence for some time that following photoexcitation to the initial Franck−Condon state of ruthenium compounds, there is very rapid relaxation to a triplet MLCT state, which is localized on a single ligand. What has not been clear is whether that localization persists for only some nanoseconds or lasts for microseconds, although the former has been considered much more likely. According to two recent reports,[27,28] such localization persists for times as long as ten microseconds, at least in ruthenium complexes about the size of **D1**. For this to be true, however, a large energy barrier must inhibit excitation hopping among ligands. Such energy barriers to excitation hopping are known in very large molecules or in rigid media at low temperature, but finding such long-lived, isolated MLCT excited states in relatively small molecules violates Kasha's rules.[29]

The existence of different ligands in heteroleptic compounds produced distinguishable emission spectra with different and distinct lifetimes. In the present case, we do not find that multiple decay lifetimes found in the dendrimers are associated with clearly distinct spectra. If there are long-lived states isolated on different ligands with different decay kinetics but with common excitation and emission spectra, then following photoexcitation, some branching ratio must exist for populating states of identical chromophores that have different lifetimes.

Our studies require two features:[1] conformations that differentiate among ligands must persist for a microsecond and[2] a high-energy barrier between states localized on different ligands. Whether a particular group after photoexcitation can have only one decay rate (albeit a rate different from decay rates in other molecules) or each molecule can have multiple rates, each associated with excitation being localized on one ligand, but affected by the other two ligands, remains unclear. For ligand-localized states, the corresponding dendrimeric emissive states can be observed. Of course, even if each molecule has distinct, long-lived, ligand-localized states, it may still be the case that in sufficiently large dendrimers, the set of states is somewhat different than in the unsubstituted parent.

(27) Glazer, E. C.; Magde, D.; Tor, Y. *J. Am. Chem. Soc.* **2005**, *127*, 4190.
(28) Glazer, E. C.; Magde, D.; Tor, Y. *J. Am. Chem. Soc.* **2007**, *129*, 8544.
(29) Kasha, M. *Discuss. Faraday Soc.* **1950**, 14.

Transient absorption spectra reveal bleaching of the MLCT band along with the transient absorption at both shorter and longer wavelengths. Isosbestic points are observed where ground-state bleaching and excited-state absorption coincide in molar absorptivity, that is, near 405 and 490 nm. There may be small variations among the four compounds, but there are no dramatic spectral shifts within the family. The point-by-point kinetic analysis used here gives good evidence from decay times that the features detected are related to the same state (or states) responsible for emission.

Of importance for our future investigations, there are no ultrafast features in either emission or transient absorption. And there is little or no electron transfer to or from surrounding solvent in the present systems on long time scales, allowing us to monitor the desired intramolecular processes directly.

5. Conclusions

Dendrimeric ruthenium complexes **D0**−**D3** show features not found in smaller homoleptic compounds, particularly with regard to luminescence decay kinetics, which are distinctly non-exponential. This establishes the existence of different conformations and different radiative and non-radiative relaxation rates. In all other aspects of their behavior, the compounds are quite similar to smaller ruthenium complexes. Their electrochemistry is the same, except that **D3** shows irreversible features; absorption spectra are familiar; emission spectra are broader but are clearly ascribed to a familiar MLCT state, which is populated in high yield and probably decays by similar pathways, except for a modest increase in decay rate. There are no extraneous ultrafast processes causing premature self-quenching of incident excitation. Therefore, we conclude that these, or closely related species, may serve as highly absorptive efficient antenna systems. Such arrays, may find practical use in photosensitization of thin film semiconductor devices, which require high densities of surface-bound dyes.

Acknowledgment. This work was supported in part by the United States Department of Energy, Office of Basic Energy Sciences, Chemistry Division.

IC800965P